ADVANCED LIGHT SOURCE BEAM DIAGNOSTICS SYSTEMS*

Jim Hinkson

Advanced Light Source
Accelerator and Fusion Research Division
Lawrence Berkeley Laboratory
University of California
Berkeley, CA 94720

October 1993

Paper presented at the 1993 Los Alamos Beam Instrumentation Workshop
Santa Fe, New Mexico, October 20-23, 1993

*This work was supported by the Director, Office of Energy Research, Office of Basic Energy Sciences, Materials Sciences Division, of the U.S. Department of Energy, under Contract No. DE-AC03-76SF00098.

ADVANCED LIGHT SOURCE BEAM DIAGNOSTICS SYSTEMS*

J. Hinkson
Lawrence Berkeley Laboratory
1 Cyclotron Road
Berkeley, CA. 94720

ABSTRACT

The Advanced Light Source (ALS), a third-generation synchrotron light source, has been recently commissioned. Beam diagnostics were very important to the success of the operation. Each diagnostic system is described in this paper along with detailed discussion of its performance. Some of the systems have been in operation for two years. Others, in the storage ring, have not yet been fully commissioned. Those systems were, however, working well enough to provide the essential information needed to store beam.

The devices described in this paper include wall current monitors, a beam charge monitor, a 50 ohm Faraday cup, DC current transformers, broad-band striplines, fluorescent screens, beam collimators and scrapers, and beam position monitors, Also, the means by which waveforms are digitized and displayed in the control room is discussed.

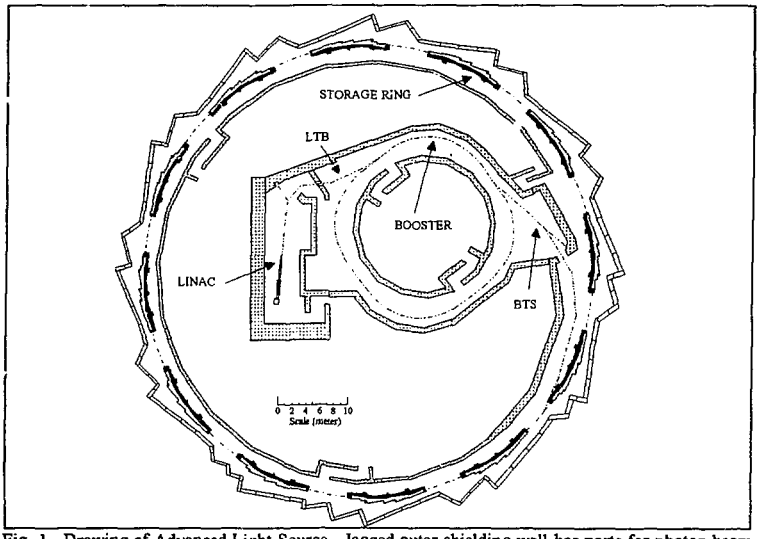

Fig. 1. Drawing of Advanced Light Source. Jagged outer shielding wall has ports for photon beam lines.

*This work supported by the Director, Office of Energy Research, Office of Basic Energy Sciences, Materials Sciences Division of the U.S. Department of Energy, under Contract No. DE-AC03-76SF00098

INTRODUCTION

The ALS (Fig 1) is a third-generation synchrotron radiation source designed for the inclusion of wigglers and undulators in the storage ring lattice. The accelerator complex consists of a 120 keV electron gun, gun-to-linac (GTL) transport line, 50 MeV linac, linac-to-booster (LTB) beam transfer line, a 1.5 GeV booster synchrotron, booster-to-storage ring (BTS) beam transfer line, and the 1.5 to 1.9 GeV storage ring (SR) which is 197 meters in circumference. The storage ring is composed of twelve curved sections, each ten meters long, and twelve straight sections approximately seven meters in length. Two straight sections are used for injection and RF acceleration. Insertion devices may be installed in the remaining ten straight sections. The entire ALS complex occupies the site once used for the 184 in. cyclotron.

The ALS construction project ended in December 1992. During the following four months the BTS and SR were successfully commissioned with most design goals being met or exceeded. The linac, LTB and booster synchrotron had been commissioned earlier. In May 1993 the accelerator was shut down for the installation of undulators and photon beam lines. In September 1993, operations resumed. During SR commissioning beam life time was dominated by vacuum chamber pressure as expected. Only a few sections of the SR vacuum chamber been baked, so pressures around the ring were relatively high. Special photon stops intercept all SR synchrotron radiation, and during early commissioning outgassing from these devices limited beam lifetime to just a few minutes. The photon stops cleaned up quickly however, and beam life time soon reached 1 hour at 100 mA. During the shutdown, all SR vacuum chamber components were baked and the titanium sublimation pumps enabled. SR pressure improved substantially. At 50 mA, life time reached 10 hours. Ultimately, at 400 mA in 250 bunches, the lifetime is expected to be 14.5 hr. Single-bunch life time will be 6.5 hours.

As commissioning progressed the maximum stored current increased daily and finally reached 460 mA, 60 mA above the design specification for 250 bunches. Single-bunch current exceeded the 8 mA specification by a factor of three. Coupled bunch instabilities at high, multi-bunch current were observed but were not as serious as expected.

Beam diagnostics in the BTS and SR were commissioned during the same four month period. The BTS beam position monitors (BPM), wall current monitor (WCM), and fluorescent screens performed as expected. The SR BPMs had some difficulties but worked well enough to help diagnose a faulty SR quadrupole magnet and optimize the beam orbit. During the shutdown the BPM problems were resolved.

What follows is a description of each ALS beam diagnostic device and a report on its performance. Table I lists accelerator parameters relevant to electron beam instrumentation.

Table I. Accelerator Parameters for Beam Diagnostics

Parameter	Storage Ring	Booster	Linac
Energy (GeV)	1-2	0.05-1	0.05
RF Frequency (MHz)	499.654	499.654	2998
Harmonic Number	328	125	-
Minimum Bunch Spacing (ns)	2	8	8
Revolution Period (ns)	656	250	-
Number of Bunches	1-250	1-12	1-20
Repetition Rate (Hz)	-	1	1-10
Maximum Average Current (mA)	400	20	125
Single Bunch Current (mA)	8	3	10
Bunch Length (2σ ps)	28-50	100	30
Tune ν_x, ν_y	14.28, 8.18	6.26, 2.79	-
Synchrotron Frequency f_s (kHz)	13.87	256-44	-

BEAM INTENSITY MONITORS

Electron beam intensity in the ALS is measured by wall current monitors (WCM), an integrating current transformer (ICT), a 50 ohm Faraday cup (FC), and DC current transformers (DCCT). Each of these devices is described in some detail and their performance shown

Wall Current Monitor (WCM)

Two identical WCMs are installed in the accelerator, one near the electron gun and the other in the 1.5 GeV BTS line. The drawing in Figure 2 illustrates their basic construction. The required break in the beam pipe is provided by an MDC stainless steel ceramic-to-metal adapter. The ceramic is 90% aluminum oxide. One of the 4.5 in. Del Seal flanges is rotatable, and the other is fixed. The beam pipe inner diameter is 2.5 in..

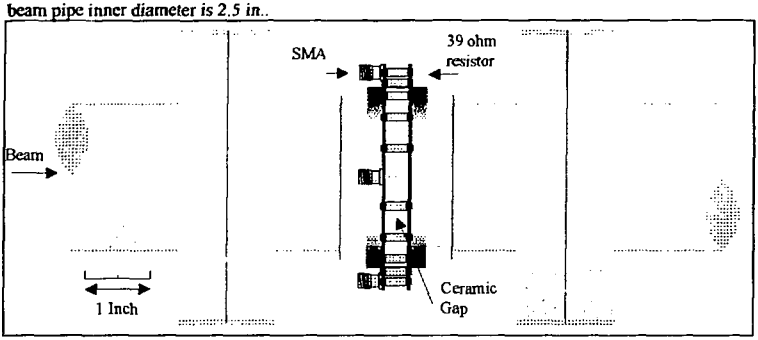

Fig. 2. Drawing of wall current monitor.

Twenty KDI microwave rod resistors are installed around the ceramic gap. Each resistor is 39 Ω giving a total gap resistance of about 2 Ω. The resistors are soldered to soft copper bands clamped around the stainless steel pipe. The vacuum side of the ceramic is metalized with a thin coating of chromium. This metalization protects the ceramic from the electron beam and somewhat damps waveguide modes. The end-to-end resistance of the coating is about 60 ohms. Four SMA coaxial connectors are used to pick off the WCM signal. The four outputs are summed in 180 degree Anzac H-9 hybrid power combiners. A 100 foot length of 1/4" Heliax cable transports the WCM signal to an SCD1000 digitizing oscilloscope for signal acquisition and remote display in the control room. Fig. 3 illustrates the electron gun WCM system diagram.

The shunt resistance, Rp, and capacitance, Cp, across the ceramic gap form a simple low pass filter determining the high frequency response of the WCM.

$$fhi(-3dB) = \frac{1}{2\pi Rp\,Cp} \qquad (1)$$

where Rp is 2 ohm. Cp is 20 pf. High frequency roll off occurs at 4 GHz.

In theory it is possible for a wall current monitor to have DC response to the beam. For this to occur it would be necessary to isolate one end of the accelerator such that all beam current is returned to the source via the beam pipe wall. In practice this would be very difficult probably unsafe to do. ALS beam pipes are grounded in many places, and these grounds put a short circuit around the WCM resistors, making DC response impossible. However, since very brief current pulses are measured, advantage may be taken of the inductance present in the ground circuits. This inductance presents a high impedance to the higher frequency components of the current pulses and forces the wall current

through the resistors. The inductance and resistance across the ceramic gap form a high pass ne defining the low frequency response of the wall current monitor

$$f_{lo(-3dB)} = \frac{Rp}{2\pi Lp} \tag{2}$$

where L_t is the total shunt inductance, 130 nHy. Low frequency roll off occurs at about 2.5 MHz.

When many gun pulses are observed the lack of good low frequency response causes a noticeable baseline tilt in the oscilloscope waveform (Fig. 4). This will be corrected with frequency compensation circuits in the future. Another addition to the WCM will be a log amplifier. During single-bunch operation of the storage ring it is important that no beam exist in adjacent beam buckets to better than 0.001. This is best achieved by adjusting the electron gun grid pulsing for a single bunch observed at the GTL WCM.

Fundamentally, the sensitivity of the WCM is about 2 V/A. The beam signal is tapped off the resistance belt at four places and summed in hybrid power combiners. This compensates beam position effects, but it complicates sensitivity. The frequency response of the wall current monitor, hybrids, and coaxial cable alter the sensitivity unequally over the beam pulse frequency range. For example, a 1 A, 10 ns beam pulse centered in the pipe develops about 2 V peak across the gap resistance. Each hybrid sums two of the signals and should provide 1.414 * 2 V at the sum port. Actually, each signal undergoes a low frequency (3 MHz to 500 MHz) attenuation of about 0.4 dB or 4.5 %. Frequencies near 1 GHz are attenuated 1 dB or 11 %. The sum of the two signals is actually 2.7 V during the flat portion of the pulse and 2.5 V at the peak of the leading edge. The two summed signals are added in a third hybrid. Now the output voltage is about 1.414*2.7*.955 or 3.6 V during the flat portion and 3.1 V at the leading edge. Lab measurements showed 3.1 V/A during the flat portion of a 10 ns pulse. The coaxial cable connecting the output hybrid to the measuring oscilloscope further reduces the pulse amplitude. Measurements of the 100-foot Heliax cable showed a low frequency attenuation of 4 % and a 20 % loss for short rise times (about 1 ns). Taking 4 % off 3.1 V/A yields about 3 V/A for long pulses (>2 ns) and about 2.5 V/A for short pulses. To sum up: Long pulses from the gun develop about 3 V/A at the oscilloscope. RF modulated pulses (2 ns or less) develop approximately 2.5 V/A.

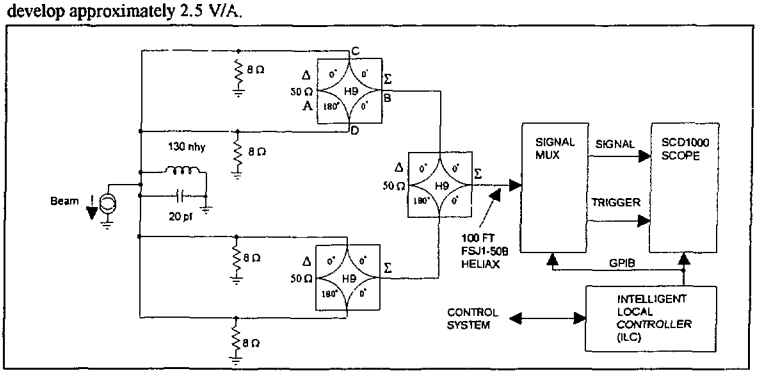

Fig. 3. Wall current monitor system connections.

Lab tests of the WCM with a single output connector revealed an unacceptable position sensitivity. Fig. 5 shows the WCM response to a 10 ns pulse in a coaxial fixture. A single connection was made to the resistor belt. The test apparatus contained coaxial tapers to smoothly

transform 50 ohms to 170 ohms near the WCM. The 0.125 inch center conductor was moved 0.5 inch off center, away from the single tap point. Approximately 5 ns were required for current distribution to equalize around the WCM. Four tap points placed symmetrically about the resistor belt were installed. The output signal from the power combiners showed considerably less position sensitivity.

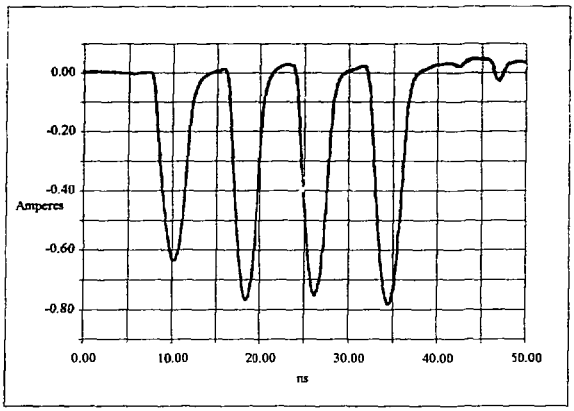

Fig. 4. Waveform taken with SCD1000 scan converter from GTL WCM.

The WCM near the electron gun measures the intensity and duration of the 120 keV electron bunches. The beam at this location consists of 1 to 20, 2.5 ns (FWHM) bunches, 8 ns apart. The beam bunches occur at 1 Hz and are typically about 1 ampere peak in amplitude. In the BTS transport line another WCM monitors the beam extracted from the booster synchrotron. Fig. 4 shows waveforms taken at the GTL. Notice the slight upward tilt in the pulse train. This is due to the limited low frequency response in the WCM.

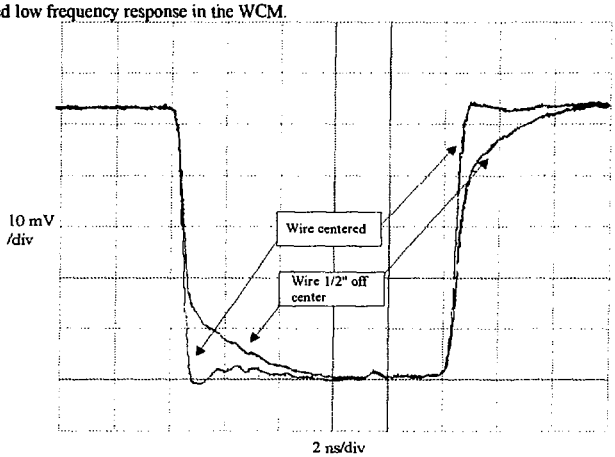

Fig. 5. WCM pulse response with centered and off-centered wire.

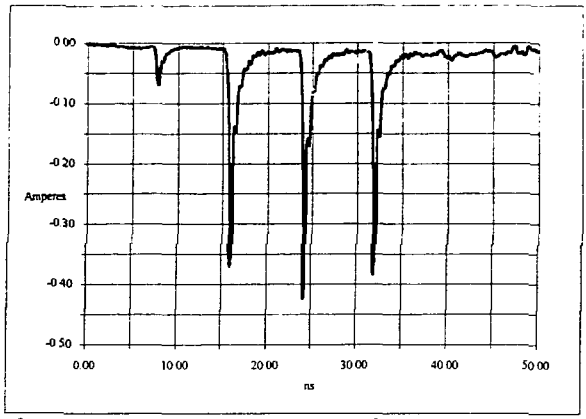

Fig. 6. Waveform taken from SCD5000 scan converter on BTS WCM.

Beam bunches in the BTS are less than 100 ps FWHM. The measurement system is not capable of accurately displaying such short bunches. The WCM, hybrid combiners, cable, and oscilloscope all reduce system bandwidth. Fig. 6 is a waveform taken at the BTS WCM. The reduced amplitude of the first bunch is probably due to energy spread in the beam and the acceptance of the booster.

Integrating Current Transformer (ICT)

The ICT [1,2] is used to measure charge in linac beam bunches. It is located at the entrance of the LTB transfer line. Fig. 7 shows the measurement system.

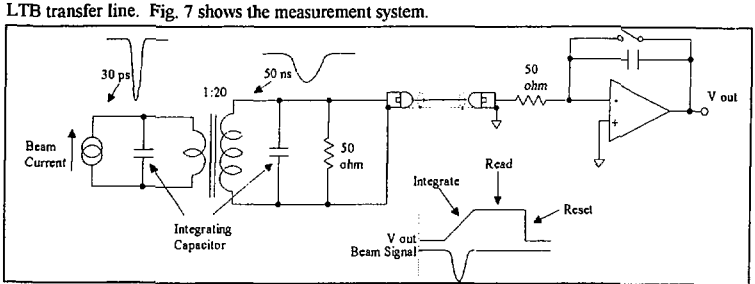

Fig. 7. Simplified diagram of integrating current transformer beam charge measurement system.

The ICT reportedly responds to bunches as short as 2 ps. Its function is to transform the very brief, high amplitude beam current pulse into a much longer and lower amplitude voltage pulse while preserving the beam charge (divided by the turns ratio). The longer pulse has considerably less bandwidth than the beam pulse and is easily measured with an oscilloscope or gated integrator. Integration by the oscilloscope or the gated integrator yields a trace amplitude or voltage proportional to beam charge. Fig. 8 shows the raw ICT output voltage and the integrated signal representing beam charge. The ICT signal was transported to the TDS 544A oscilloscope via 100 feet of 1/4 inch Heliax. Signal integration was performed in the oscilloscope digital signal processor. Scaling to nano coulombs was performed in an Excel spreadsheet. In the future, the ICT voltage will be integrated and scaled in an intelligent local controller (ILC) for control room display. The ILC is the low-level input/output module for the ALS control system.

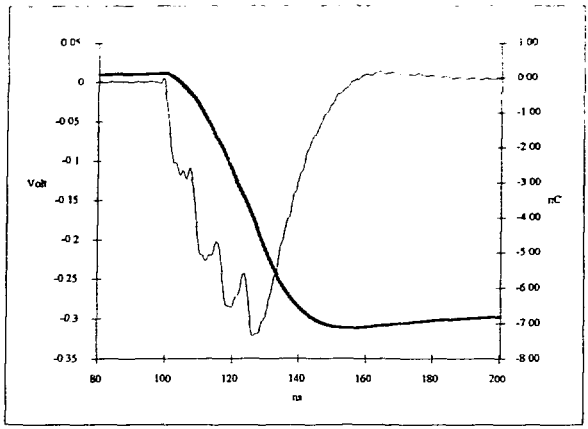

Fig. 8. ICT raw output and integrated voltage (heavy line) with four linac beam bunches. Data taken with a TDS 544A oscilloscope.

Faraday Cup

A 50 ohm Faraday cup is installed in a short diagnostics beam line off the LTB beam line. The cup is used to measure the total charge of the linac beam having passed through an analyzing magnet. A passive, impedance matched RC network integrates the cup output voltage for measurement by a 2440 digitizing oscilloscope. The 2440 waveform is displayed in the control room. Fig. 9 illustrates basic cup construction and Fig. 10 the beam charge measurement system. An interesting feature of this cup design is the ceramic break. It supports the coaxial center conductor and permits having air as the transmission line dielectric rather than vacuum. This means an ultra-high vacuum coaxial feedthrough is not needed for the cable connection.

Two sub-harmonic bunchers and one 3 GHz buncher in the GTL beam line compress the 2.5 ns electron gun beam bunches longitudinally for acceptance by the linac. Most efficient acceleration occurs when a single bunch is accelerated in one S-band beam bucket. The aim in using an impedance matched Faraday cup was to permit direct observation of linac beam longitudinal bunch shape in order to permit optimum buncher tuning. In order to accomplish this a single-shot measurement system having a rise time of 100 ps or less was required. The cup signal was connected via 60 feet of 1/2 inch Heliax to the input of an SCD5000 scan-converter oscilloscope having a single-shot bandwidth of about 5 GHz. The combined rise time of the cable and SCD5000 is about 100 ps. Unfortunately, the cup rise time is 300 ps. This is due to the lumped capacitance of the ceramic break at the entrance of the cup. Although the cup does not have the desired frequency response, it is still useful. Energy spread in multi-bunch linac beam is measured with the cup and an adjustable-gap beam collimator located between the cup and the analyzing magnet.

Another attempt at observing linac beam micro-structure was made. Four 11 mm diameter BPM buttons[3] were installed in the beam pipe near the cup. The buttons were mounted flush to the inside of the pipe wall. The waveform observed from a single button is shown in Fig. 11. The measurement results were encouraging. The bunching action of the 125 MHz subharmonic buncher could clearly be seen as its RF level was adjusted. The upper trace in Fig. 11 shows a properly bunched beam. The lower trace indicates beam in several adjacent S-band buckets with the buncher RF off. The ringing after the bunched beam has not been investigated. It could be due to wake fields from upstream beam-pipe discontinuities, button transient response, or ringing in the Heliax cable. Similar Heliax cable ringing stimulated by short pulses has been observed before.

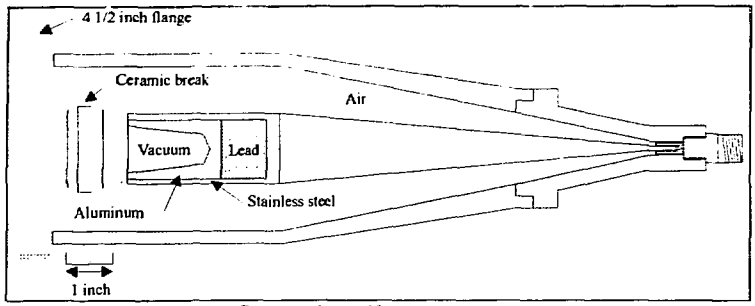

Fig. 9. 50 MeV Faraday cup. Connector is type N.

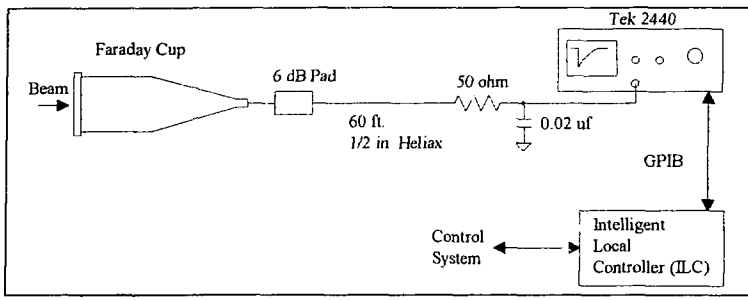

Fig. 10. Faraday cup beam charge measurement system.

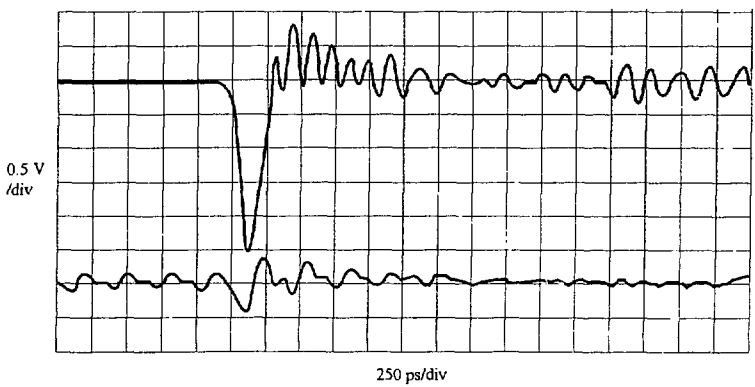

Fig. 11. 11mm button response to linac beam. Upper trace: 125 MHz buncher on. Lower trace: 125 MHz buncher off.

DC Current Transformer (DCCT)

The most accurate method available for non-destructive measurement of the DC component of a circulating beam is with a DC current transformer or DCCT. Other names for these devices are parametric current transformers[2], second-harmonic magnetic modulators, and zero-flux current transformers. DC transformers as such do not exist of course. A time-changing magnetic field is required for transformer coupling. But from a "black-box" point of view, the DCCT does appear to couple DC fields.

Fig. 12 is a simplified diagram of a DCCT. A high-permeability, tape-wound toroidal core having several separate windings encircles a break in the beam pipe. One winding of the core is excited by a square wave modulation current driving the core into positive and negative saturation (55 Hz in the booster and 7 kHz in the storage ring). A secondary or "sense" winding couples to the flux produced by the modulation current. The voltage waveform on this winding is normally symmetrical about zero. It's Fourier components consist of only the modulation fundamental frequency and its odd harmonics. This is the situation when no beam or external magnetic field is present. When a foreign magnetic field (from the beam or anywhere else) couples to the core the sense winding voltage is no longer symmetrical about zero. It is skewed slightly positive or negative depending on field polarity. A synchronous detector operating at twice the modulation rate (the second harmonic) samples the sense winding voltage whose average value is now non-zero. After filtering the resulting error voltage is amplified and fed back to another winding, canceling the offsetting flux and restoring the sense winding voltage symmetry. This means the core operates at zero DC flux. By operating at zero flux, the DCCT guarantees high measurement linearity. Average beam current is derived by measurement of voltage dropped across a precision resistor in the feedback current path. Since the transformer turns ratio is exactly known, an exact measure of beam current is provided.

Low frequency fields from the beam penetrate the ALS aluminum beam pipe. In principle it would be possible to sense these fields with an appropriate detector, but "foreign" currents flowing along the beam pipe would interfere with the measurement. It is necessary to shunt these currents away from the detector in order to measure beam current only.

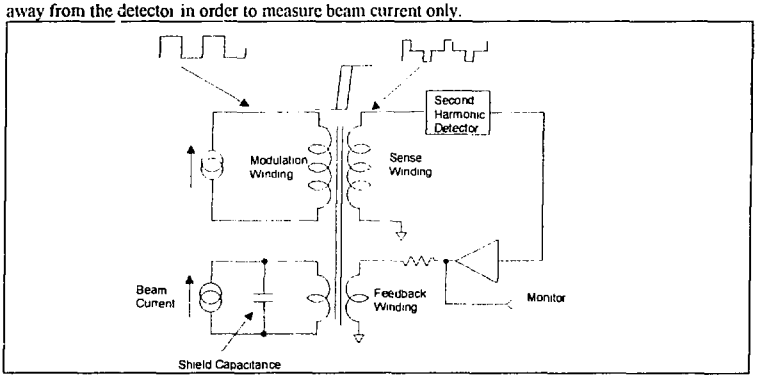

Figure 12. Simplified diagram of a DCCT

Without a break in the aluminum beam pipe a DCCT would not function because the beam pipe (and its many grounds) would form a shorted turn around the core, disrupting its function. In all DCCT accelerator applications it is necessary to install a beam line insulating gap and a DCCT shield. Figure 13 is a simplified drawing of the shield in the ALS storage ring.

The shield has three basic functions. The first is to provide a break in the beam pipe forcing low-frequency beam wall current to encircle core. See the dashed line in the illustration. Note that the core does not have to be placed directly over the ceramic insulator or the gap. The second function of the shield is to provide a shunt path for foreign currents flowing along the outside of the

beam pipe. These currents do not couple to the core. The last purpose of the shield is to prevent RF fields from being radiated. Both ALS DCCT shields are "separate function" devices. That is, there are two gaps, one to isolate vacuum and one to break the low-frequency beam current path. The beam moves through an inner pipe called a waveguide in Fig. 13. This pipe has vacuum on both sides and is isolated from one end of the shield by a 0.25 mm gap. The high gap capacitance provides a low reactance path for the high-frequency components of the wall current. Ideally no RF fields reach the core. In practice, both shields resonate at about 40 MHz. It is very difficult to build a shield that cannot be resonated in some mode by the intense, short beam bunches.

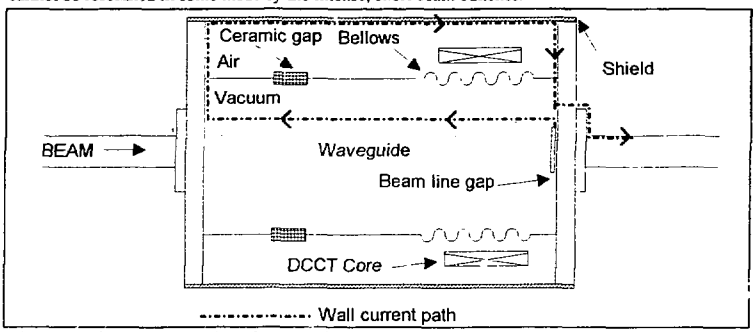

Figure 13. Simplified drawing of storage ring DCCT shield.

Vacuum isolation is provided by an MDC ceramic gap. A bellows in the outer pipe relieves stress on the ceramic. In the storage ring DCCT shield a heater (not shown) is installed for vacuum bake out. Thermocouples under the core in the storage ring DCCT are used to insure that core temperature does not exceed 80 degrees Celsius during bake out. Permanent core damage will result if that temperature is exceeded. For that reason the core is water cooled during baking.

The booster DCCT[4] works reliably and is routinely used to measure booster beam at levels up to 20 mA. The DCCT waveform is observed on a control room computer display. The DCCT signal contains an objectionable amount of ripple at the core modulation frequency (55 Hz). The ripple amplitude is equivalent to 0.5 mA beam current. It is believed the ripple is due to the effect of RF filters installed in the DCCT cables. Without the filters the DCCT electronics were badly upset by beam-induced RF picked up in the core windings. The cores are not shielded, and as luck would have it, the shield resonates at the 10th harmonic of the booster revolution frequency (4 MHz). A single bunch circulating in the booster has strong frequency components at 40 MHz. Even with the RF filters in place, single-bunch beam still upsets the sensitive DCCT electronic feedback circuits. Core shielding will be improved. Also, the ripple will be investigated and removed if possible.

The SR DCCT[5,6] has three outputs; Low Pass Filtered, Wide Band, and di/dt. The control system monitors the filtered and di/dt outputs. Fig. 14 below shows a DCCT computer display. This application displays DCCT measured current or the di/dt signal, and calculated beam lifetime. It also indicates vacuum pressure around the storage ring. The pressure fluctuates with current level. Since all storage ring vacuum components were baked during the recent shutdown, the non-beam operating pressure has fallen to about 2 e-10 torr. With 100 mA beam the pressure rises about 1 decade.

The DCCT wideband and di/dt outputs are displayed on an oscilloscope. The di/dt signal is useful for measuring beam stacking current shot-to-shot and for quick display of beam life time gain or loss as the storage ring lattice is tuned.

During storage ring commissioning when new intensity records were being set every day, there was some concern whether the DCCT was reporting the correct current. The absolute accuracy of the DCCT was checked by a measurement of heat produced by synchrotron radiation in a photon stop. There is a known relationship between the average current in the machine and the intensity of

synchrotron radiation. Since a known fraction of the radiation fan is intercepted by the photon stop, it was a fairly simple matter to measure the temperature rise in the photon stop cooling water and calculate the average beam current. With 300 mA in the ring as measured by the DCCT, the experimental data indicated 260 mA. Table 2 shows electrical specifications for the two DCCTs

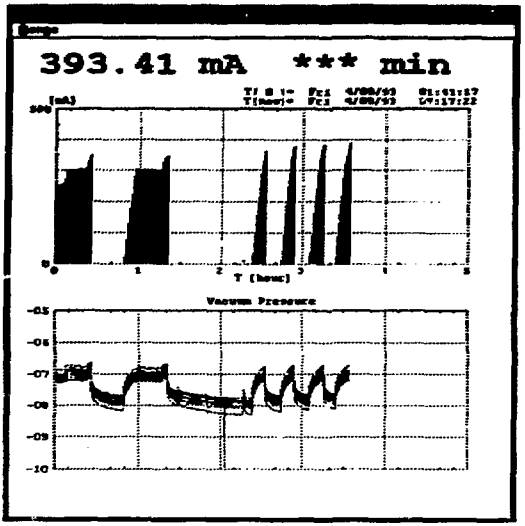

Figure 14. Image of ALS control system SR DCCT and pressure display.

Table 2. ALS DCCT Specifications

DCCT Specification	Storage Ring	Booster
Manufacturer	Bergoz	Holec
Range	A: 0 to +/- 1A B: 0 to +/- 10 mA	0 to +/- 100 mA
Output (full scale)	0 to 10 V	0 to 10 V
Frequency Response	DC to 100 Hz (LPF) DC to 20 kHz (HF)	DC to 20 kHz
Accuracy	+/- 0.1% full scale	+/- 1% full scale
Resolution	+/- 5 μA	+/- 0.5 mA
di/dt Sensitivity	10 mA/sec/Volt	NA

BROAD BAND STRIPLINE MONITORS

Three styles of striplines are installed in the ALS. In the LTB and BTS beam transport lines, arrays of four striplines arranged for X and Y beam position monitoring[7] are installed. These are conventional striplines, 150 mm long, and shorted to the beam pipe on the downstream end. Striplines in the SR are currently used to drive the beam during betatron fractional tune measurements. The upstream end of these kickers may be used for beam monitoring. In the future these striplines will be used to damp transverse beam oscillations in a fast, bunch-by-bunch feedback system[8]. Some unusual slotted line beam pickups and kickers have been installed in the booster beam tune measurements. These devices are discussed next. A cut away drawing of the booster stripline is shown in Fig. 15.

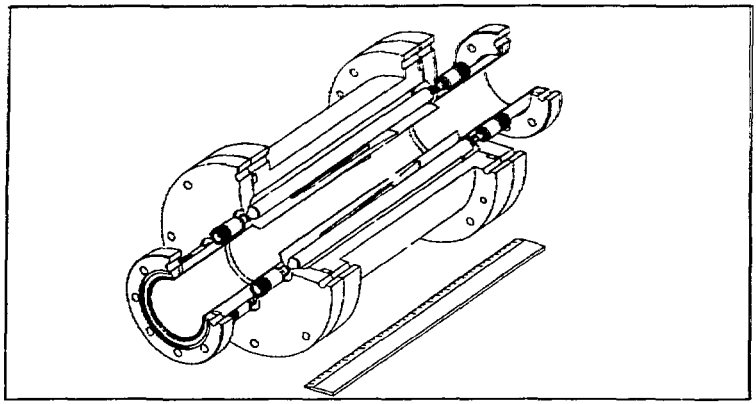

Figure 15. Cutaway view of booster slot-coupled stripline monitor. Connectors are type N. Exponential slots cut in a thin wall brass insert define beam coupling to coaxial lines.

In designing the booster striplines[9] (called Traveling Wave Electrodes, or TWEs) our aim was to develop broadband pickups having smooth frequency response instead of the sin(x) response characteristic of typical striplines. Exponentially tapering stripline width and wall spacing over its length yields the desired response. However, holding mechanical tolerances in such a geometry is difficult. Instead, a slot-coupled pickup in which beam coupling to a 50 ohm transmission line is determined by dimensions of a machined slot was chosen. The slot is exponentially tapered over its length and yields the same response as a tapered line. Fig. 16 shows the measured frequency response and the beam response of tapered, slot-coupled stripline. The coupling impedance of the stripline is low, only 0.6 ohm (measured pulse response).

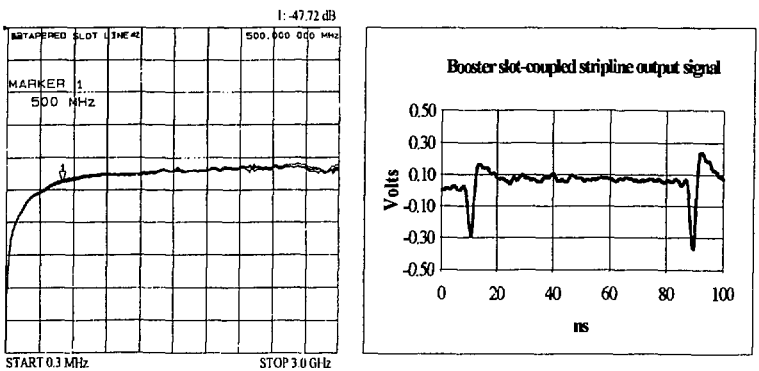

Figure 16. Measured frequency response of four tapered, slot-coupled striplines (left). Time response to beam bunches of single stripline (right) measured with an SCD5000 scan converter.

The slot-coupled stripline construction is simple and sturdy. The 63 mm beam aperture was drilled through the center of a solid, cylindrical aluminum block. Four holes 32 mm in diameter were drilled 44 mm off the center of the beam axis each 90 deg apart. The four holes intersect the beam pipe hole forming 16 mm apertures the full length of the block. Aluminum rods inserted into the four holes form 50 ohm coaxial lines. The slotted thin-wall tube fits snugly into the beam aperture. Coaxial vacuum feedthroughs support the coaxial line center conductors.

There are two slot-coupled stripline assemblies in the booster synchrotron situated an odd-number of betatron wavelengths apart. The four outputs of each stripline assembly are connected to 180 degree hybrid power combiners via 80 ft. phase-matched Heliax cables. The hybrids deliver Δx, Δy, and a sum signals for display on a spectrum analyzer or oscilloscope. A third stripline without tapered slots is used as a beam kicker. The pickups and kicker are part of a fractional tune measurement system which includes a spectrum analyzer and tracking generator. While the pickups have been useful for broad band beam measurements, the kicker has not functioned well. Because the booster sextupoles are not energized, the beam tune spread is too great for low-level transverse excitation. With over 100 watts applied to the kicker, no resonant beam response has been observed. Since adequate booster beam is accelerated with the sextupole magnets off, and because alternate methods exist, there is no requirement for tune measurements using the stripline kicker. Booster betatron tune is easily measured with the beam position monitors to a resolution of 0.01. At injection fractional tune in X and Y is found by performing an FFT on data from 1024 sequential turns. At higher energies, when the beam is damped, the beam is horizontally excited with the extraction kicker at low fields, and the BPMs are used once more. Transient beam phenomena are studied with a Tektronix 3052 real time spectrum analyzer. BPM base band video signals may be measured directly. Signals from the striplines are down converted in an HP71210C spectrum analyzer before measurement by the 3052.

FLUORESCENT SCREENS AND TV

Fluorescent screens and TV cameras are installed in 22 locations in the ALS. Their function is to display beam size, position, and current density. In all but two locations screens supplied by Morgan Matroc[10] in the U.K. are installed. These screens are referred to as "Chromox 6". They were purchased in 75x75 mm squares, 1 mm thick. Chromox 6 is composed of very pure alumina doped with 0.5 % chrome sesquioxide and is pink in color. Johnson[11,12] reports the fluorescence is peaked at 690 nm. The spectral response has not been measured at the ALS. The fluorescent light decay time constant has been measured to be approximately 20 ms.

The experience with Chromox 6 at the ALS has been generally satisfactory. It appears to be sturdy. None of the screens have shown evidence of radiation damage after three years in service. The material is bakable and UHV compatible. Standard ceramic cutting techniques were used to shape the material. Scales and identification labels were marked on the screens with ordinary pencil lead.

Chromox 6 will reportedly produce enough light for a normal vidicon camera with as little as 10^9 electrons per cm sq. striking the screen. A typical ALS electron contains 1 nC or about 6 times that required for a usable TV image. In our case the optical components and TV camera used made observation of a single bunch difficult at first.

A typical screen installation includes a electrically controlled pneumatic actuator, a Fairchild CD5000 CCD camera, a 70-210 mm, f5.6 zoom lens, a lead shield, and an incandescent lamp to illuminate the screen through a quartz vacuum window. The TV signals are multiplexed to control room monitors and a frame grabber. HP3488 switch controllers connected to the accelerator control system via the IEEE 488 buss do the video switching.

The Fairchild cameras were chosen because of their rugged construction and small size. Four small CCD heads may be controlled by a remote master, up to 25 feet distant. These cameras are designed for normal ambient lighting conditions and use ordinary C-mount TV lenses. There have been some camera failures. None of the failures can be attributed to ionizing radiation.

Zoom lenses rather than fix-focus lenses were chosen to optimize image size and simplify the optical setup. They are ordinary 35 mm camera lenses fitted with C-mount adapters for TV use. Lens extenders are installed to permit close focus. Because the lenses are not particularly fast and extenders are used, light collection is not optimum. Another reduction in transmitted light was caused by rotatable polarizers which were used as remote controlled light attenuators. Since the CCD cameras do not have automatic gain control, the polarizers were required to normalize light levels for different bunch patterns. The dynamic range of the polarizers is 300 to 1. It was assumed radiation would damage lenses over time. Expensive motorized lenses were deliberately not used. Early in the commissioning of the linac and LTB lines all polarizers were removed because their minimum attenuation was too high. So far, none of the lenses have shown signs of radiation damage.

A visiting colleague[13] reported Chromox 6 produces strong infrared. Acting on his advice, we removed IR filters from the CCD cameras. The image intensity increase significantly (four f-stops) Fig. 18 shows the spectral response of the CCD sensor alone and the camera response (using the same CCD) with the IR filter in place. The filter shifts the camera response to shorter wavelengths by over 200 nm.

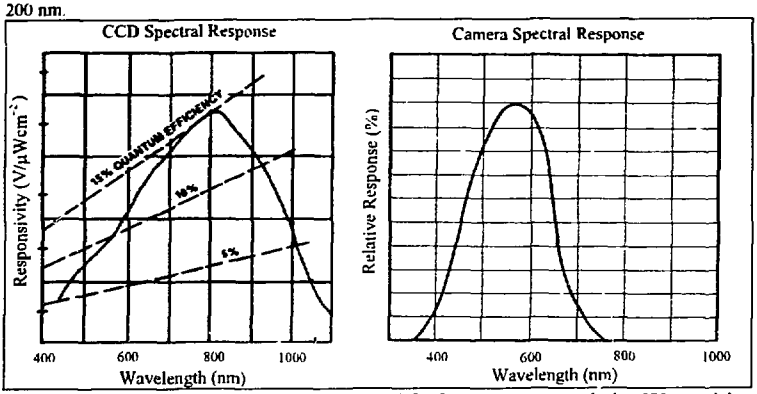

Figure 18. CCD spectral response peaked at 810 nm, left. Camera response peaked at 575 nm, right.

The TV lens apertures have been adjusted for linear camera response with between 1 and 6 beam bunches. Good linearity is required for an emittance measurement system[14] that includes a frame grabber, a screen image, and analysis software.

The incandescent lamps that illuminate the screens produce strong infrared. Electronic dimmers were installed on the lamps to balance screen illumination with the light produced by the beam striking the screens. The polarizers were tested with infrared light to determine if they could still be used. Using a simple IR LED and a camera without its filter, we determined the polarizers had little effect on the IR light intensity. If an acceptable infrared polarizer can be found, the attenuators will be reinstalled. Until then the camera video will be saturated with more than 6 beam bunches.

The Chromox screens are good insulators. They are installed in aluminum picture-frame holders and do not have conductive substrates or coatings (apart from the scale). In the GTL line where beam energy is only 120 keV the Chromox screens stopped the beam completely. Consequently, the screens charged and flashed after several pulses of beam. The image they produced was not usable. They were replaced with screens made from zinc oxide sprayed on a stainless steel plate. These screens are not as robust as Chromox 6 and do not have the good vacuum properties, but they do not have discharge problems.

BEAM COLLIMATORS AND SCRAPERS

Beam collimators are installed in the LTB transport line. Two collimators which define a beam aperture horizontally and vertically are located on the branch line going to the booster. A single horizontal collimator was installed in the diagnostics line going to the coaxial Faraday cup. This collimator was used in conjunction with an upstream analyzer magnet and the cup to study beam energy spread in the linac beam. This collimator has been removed to make space for diagnostic development.

The remaining collimators define the 50 MeV linac beam dimensions with 0.5 inch tantalum jaws. Compressed air is forced through the jaws to remove heat. The jaws are positioned with precision lead screws driven by stepper motors, and position is determined with absolute position encoders[15]. Minimum step size is 10 microns. A simplified drawing of a collimator is shown below.

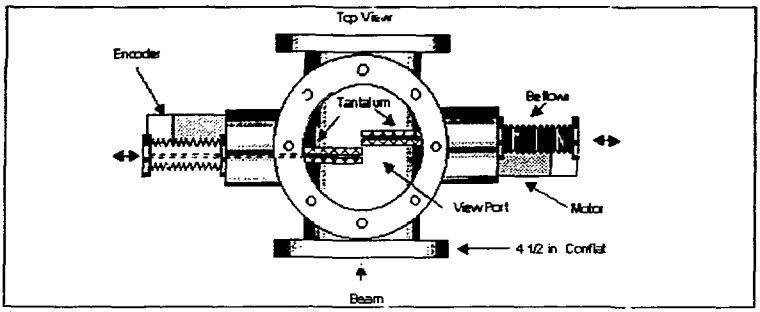

Figure 19. Drawing of single axis beam collimator.

The stepper motors and encoders in the booster branch line have worked well for two years. The encoders in the diagnostics line failed three times before that collimator was removed. In all cases the cause of failure was an LED in the optical encoder. Since the encoders were installed in the beam plane, radiation was suspected as the reason for failure. However, the measured dose rate was not high enough to confirm our suspicions.

Beam Scraper

A beam scraper with three blades is installed in a storage ring straight section reserved for a short wiggler. The function of the scraper is to permit investigation of the storage ring dynamic beam aperture by restricting the physical aperture. It is also used to gracefully reduce stored beam intensity. The location of the scraper is upstream of an area with especially thick shielding.

A cut away view of the scraper is shown in Fig. 20. Only three blades are used. Synchrotron radiation on the unused side prohibits installation of a fourth blade. Control of scraper blade position is accomplished with MDC linear motion feedthroughs and Compumotor stepper motors. Motor counts are used to calculate position. Absolute position at the limits of travel is determined with optical limit switches. RF contacts on the blades insure that scraper beam impedance is low when the blades are retracted.

BEAM POSITION MONITORS

The ALS electron beam position monitors (BPM) were fully described in another paper[7]. A brief description is included here to acquaint the reader with the basic techniques used at the ALS to obtain beam position. BPM pickups are installed in 96 locations in the storage ring, 32 places in the booster synchrotron, and at 22 other locations in beam transport lines. A block diagram of a storage ring BPM electronics system is shown in Fig. 21.

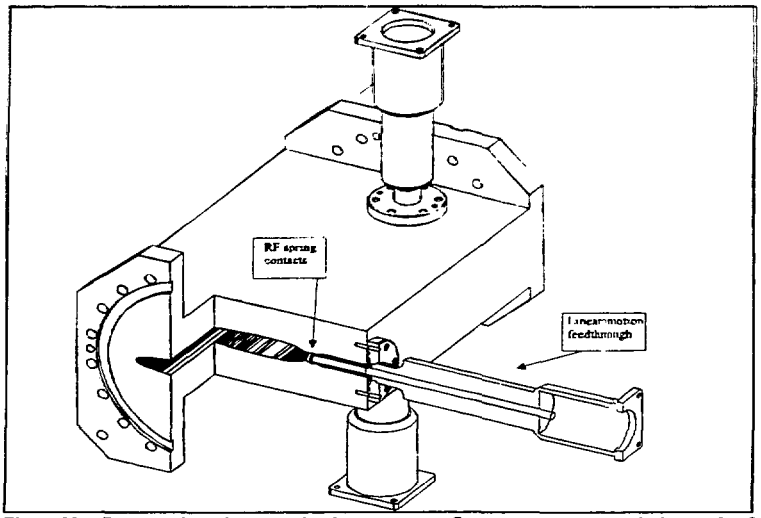

Figure 20. Cutaway view of storage ring beam scraper. Stepper motors are attached to ends of motion feedthroughs.

Each BPM pickup array consists of four button-type electrodes (SR and booster) or four striplines (GTL, linac, LTB, and BTS). The pickups are connected to the electronics bins via FSJ4-50A Heliax coaxial cable. This cable provides 100% shielding, high stability, and low loss. In the receivers the 500 MHz component of the bunched beam spectrum is selected and mixed down to 50 MHz intermediate frequency (IF). A broad band, pseudo-synchronous detector converts the signals to base band video. The detected signal is fed to three circuits, a video monitor, a fast analog-to-digital (A/D) converter, and a 1 kHz low-pass filter. The filtered signal is digitized for calculation of beam position by the difference-over-sum method. These calculations are performed by the on-board Intelligent Local Controller (ILC, the basic input-output module for the ALS computer control system). The fast A/D data are fed to first-in-first-out (FIFO) memory where up to 1024 turns of beam data are stored. The linac and transport line BPMs do not have fast A/Ds or FIFO memory.

When the fast digitizers are stopped by a halt trigger, the turn-by-turn data are recovered from one or all BPMs in the booster or storage ring. The data include raw voltages from the four channels or the calculated X and Y positions for each turn. These data are useful for tune measurements, single-shot closed orbit measurements, and other transient beam phenomena. Early in the storage ring commissioning process there was difficulty getting the beam to make a single turn with nominal magnet current settings. The ring was being run without the high power RF systems at that time. Hundreds of turns were expected before the beam orbit decayed. Orbit data were taken from the BPMs and compared with the lattice model. The results of this work[16] predicted certain magnets could be responsible for the orbit distortions. Careful visual inspection of a suspect quadrupole revealed shorted turns. The short was quickly repaired and beam orbited as expected.

The single-turn response and multi-turn storage feature of the BPMs was intended to be used as an aid in determining causes for anomalous beam loss in the storage ring. It was believed the cost of this feature would be offset by the time saved in troubleshooting an intermittent storage ring. This feature was included in the booster BPMs to test its usefulness. The fast A/Ds were not intended to be used as accurate BPMs. The accuracy of the fast circuits is about 1 mm. The dynamic range is small, equivalent to only 5 mm. On the first day of storage ring injection beam oscillations greater than 10

mm were observed. The dynamic range and accuracy of the fast digitizers may be improved with a better peak detector and error correction.

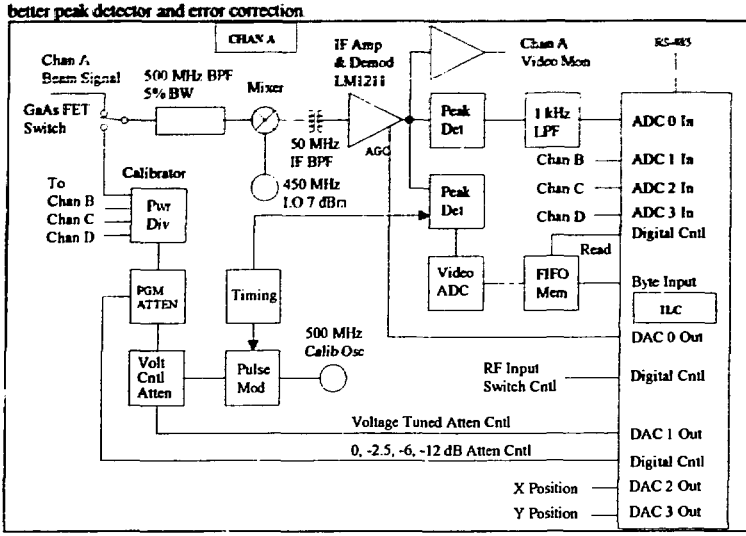

Fig. 21. Block diagram of a single channel of the storage ring BPM.

The slow, more accurate circuits in the BPMs are required to measure beam position with 30 micron repeatability and 10 micron resolution. In order to accomplish this, many system offsets must be compensated. The storage ring BPM pickups and cables are not deliberately matched. Consequently the electrical center of the BPMs is shifted from zero. The graphs in Figs. 22 and 23 show the measured offsets. The offsets were determined by measurement of the transmission between buttons[17]. The cables were included in the measurements. The average X offset is 0.3 mm. The average Y offset is 0.35 mm. Offsets exceeding 1 mm are excessive and must be investigated. Since the BPM electronics has a receiver for each button, there are differential gain and linearity offsets to compensate. Additionally, the detectors may have small DC offsets. Each storage ring BPM has internal calibration and error correction capability. The error correction sequence goes as follows: The gain of the four receivers is set manually for a 90% full scale reading in the channel with the largest signal. The calibration sequence is started and is fully automatic. The receiver front ends are switched from the beam signal inputs to the calibration inputs. At first the calibrator is turned off. DC offsets are measured and noted at this point. Next, the calibrator level is adjusted for 90% full scale in the channel with highest gain. Differences in detected signal levels are noted. The calibrator level is now reduced in precise steps as the detected voltage is noted at each step. From these data detector linearity correction coefficients are calculated. All subsequent beam measurements are corrected for DC offset, detector non linearity, and button electrical zero offsets. The net effect of this has been measured in the lab on a few BPMs. Over a 10 dB range the linearity correction scheme is effective to about 50 microns.

Currently setting BPM gain is a tedious process. All 96 of them must be dealt with individually. Automatic acquisition of the beam signals is possible but has not been implemented. A future upgrade to BPM software will include automatic gain control. BPM data are now available to the control system at 1 Hz in synchronism with beam injection. More software upgrades integrating a

BPM timer will make 10 to 20 Hz possible. In lab tests BPMs averaged 4 signals 50 times and reported position at 30 Hz.

Lately beam is routinely stored for hours, and the BPMs are used to study the storage ring. One method involves taking difference orbits. A closed orbit scan is taken, and all numbers are set to zero. Subsequent scans normalized to the previous reading show beam motion. This is done to test magnets and measure dispersion. The most important function of the BPM system is to reliably report the absolute position of the beam to 30 microns over a 40 dB dynamic range. That has not yet been demonstrated. A program of methodical evaluation of the BPMs has begun.

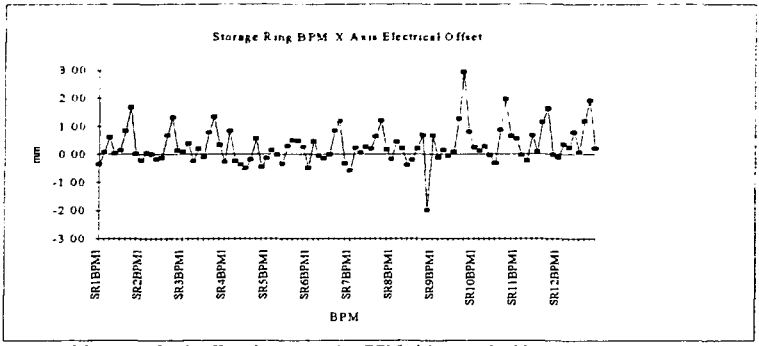

Fig. 22. Measured X-axis offsets in storage ring BPM pickups and cables.

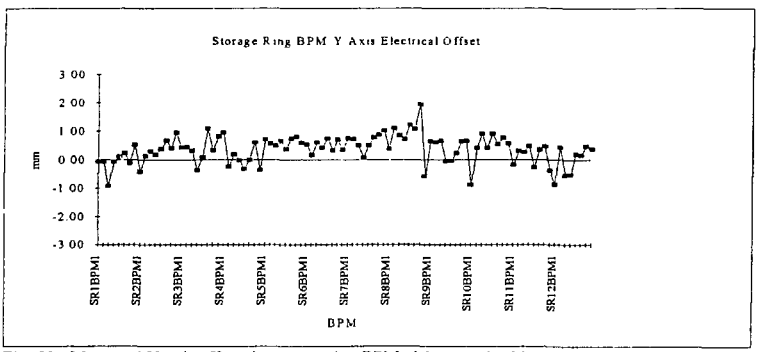

Fig. 23. Measured Y-axis offsets in storage ring BPM pickups and cables.

INSTRUMENT CONTROL AND WAVEFORM DISPLAY

Many waveforms are routinely observed in the control room. The time base for these waveforms may vary from milliseconds to nanoseconds. In order to minimize the number of coaxial cables from accelerator systems to the control room, remote digitizing oscilloscopes were installed. Nine Tektronix 2440 digitizers and one SCD1000 scan converter are used to collect the waveforms around the accelerator. Signals are multiplexed into the oscilloscopes with HP3488 switch controllers. The switch controllers are fitted with relay modules appropriate to signal bandwidth. ILCs with GPIB

interfaces allow control of the oscilloscopes and multiplexers via the accelerator control system. A custom software application operating at first under OS2 and now under MS Windows is used to select and display waveforms. The same application allows the user limited control of the oscilloscopes. Waveforms are updated at about 3 Hz. Complete interactive control of remote instruments via the control system and commercial graphical instrument control software is being explored.

TUNE MEASUREMENTS

Storage ring betatron tune may be measured with the BPMs or the fractional tune measurement system. The fractional parts of ν_x and ν_y are measured with an HP71210C spectrum analyzer equipped with a tracking generator in those situations when the beam is well damped. Transverse beam oscillations must be excited to be observed on the analyzer. In other cases when coherent beam oscillations are present, no beam excitation is required and the 3052 analyzer may be used.

The present tune measurement system is temporary. The beam pickups and kickers are part of the transverse bunch-by-bunch beam damping system which is being installed. The vertical and horizontal kickers are driven by 35 watt amplifiers having a bandwidth of 10 kHz to 300 MHz. The kicker stripline bandwidth is DC to 500 MHz. The transverse shunt impedance of the kickers is 10 kΩ at zero frequency and falls to zero at 500 MHz. Both kickers are driven simultaneously.

Resonant response of the beam is detected by LEP button pickups. These buttons[18] have been modified to eliminate resonance near 4 GHz. Their -3dB low frequency response occurs at about 500 MHz, and their coupling impedance is approximately 1 Ω. The output of the four buttons is processed in 180 degree hybrid power splitters yielding ΔX, ΔY, and sum signals. The ΔX and ΔY signals are added in another hybrid and sent to the control room analyzer.

Synchrotron tune measurement is performed by observing the hybrid sum signal on the spectrum analyzer. No beam excitation is needed. Synchrotron side bands are observed approximately 9 kHz on either side of any rotation harmonic within the bandwidth of the measurement system.

CONCLUSION

Most ALS instrumentation is working well and reliably. Some systems require minor improvements. The storage ring BPMs are still being evaluated. Currently instrumentation design efforts are focused on photon beam position monitors.

ACKNOWLEGEMENTS

I am pleased to acknowledge the efforts of some LBL colleagues who made very significant contributions to the ALS beam diagnostics effort. Jim Johnston has for 5 years been working on the design, fabrication, testing, installation, and commissioning of the BPMs. Al Geyer coordinated fabrication, documentation, and installation of all beam diagnostics and major parts of the vacuum system electronics. Michael Fahmie designed the timing system which is the heart beat of the ALS. Mike Chin made it possible for the control system to communicate with GPIB controlled instrumentation and also created the software used to display oscilloscope waveforms in the control room. Both Chin and Fahmie were also chiefly responsible for the hardware implementation of the control system ILC.

REFERENCES

[1] Integrating Current Transformer BERGOZ, 01170 Crozet, France

[2] K.B. Unser, "Design and Preliminary Tests of a Beam Intensity Monitor for LEP," Proc 1989 IEEE PAC, 89CH2669-0, pp. 71-73

[3] ESRF BPM Button, Meta-Ceram, 94800 Villejuif, France

[4] Zero Flux Current Transformer, HOLEC Model SHES 1000, 7550 aa Hengelo

[5] Parametric Current Transformer, BERGOZ, 01170 Crozet, France

[6] K. B. Unser, "The Parametric Current Transformer, a Beam Current Monitor Developed for LEP," AIP Conf. Proc. No. 252, Accelerator Instrumentation, Particle and Fields Series 46, pp. 266-275, 1991

[7] J. Hinkson, "Advanced Light Source Beam Position Monitor," AIP Conf. Proc. No. 252, Accelerator Instrumentation, Particle and Fields Series 46. pp. 21-42, 1991

[8] W. Barry, C.C. Lo, Glen Lambertson, "Electronic Systems for Transverse Coupled-Bunch Feedback in the ALS," these proceedings

[9] J. Hinkson, K. Rex, "A Wide Band Slot-Coupled Beam Sensing Electrode for the Advanced Light Source (ALS),", Proc. 1991 IEEE PAC, 91CH3038-7 pp1234-1236

[10] Chromox Screens, Morgan Matroc Limited, Surrey KT80QZ, England

[11] C. D. Johnson, "Limits to the Resolution of Beam Size Measurement From Fluorescent Screens Due to the Thickness of the Phosphor,", Single Pass Collider Memo CN-366, 1988

[12] C. D. Johnson, "Technical Notes on Alumina Ceramic Fluorescent Screens", Sept. 1989, unpublished

[13] J. C. Denard, private communication to author

[14] J. Bengtsson, W. Leemans, T. Byrne, "Emittance Measurement and Modeling of the ALS 50 MeV Linac to Booster Line," Presented at the IEEE PAC, Washington, DC, May 17-20, 1993, and to be published in the Proceedings

[15] Parker, Compumotor, indexers, motors, and position encoders

[16] J. Bengtsson, M. Meddahi, "Elementary Analysis of BPM Data for the ALS Storage Ring," LBL CBP Tech Note 003, March 1, 1993

[17] G. Lambertson, "Calibration of Position Electrodes Using External Measurements," LBL ALS Internal Note LSAP05, 1987

[18] W. Barry, "Broad-Band Characteristics of Circular Button Pickups," AIP Conf. Proc. No. 281, Accelerator Instrumentation, Particle and Fields Series 52. pp. 175,184, 1992